Journal of Applied Polymer Science

Electrical behavior of dual-morphology polyaniline

Anil Kumar,[1] Lokesh Kumar Jangir,[2] Yogita Kumari,[2] Manoj Kumar,[2,3] Vinod Kumar,[1,4] Kamlendra Awasthi[2,3]

[1]Department of Metallurgical and Materials Engineering, Malaviya National Institute of Technology, Jaipur 302017, India
[2]Department of Physics, Malaviya National Institute of Technology, Jaipur 302017, India
[3]Centre for Energy and Environment, Malaviya National Institute of Technology, Jaipur 302017, India
[4]Materials Research Centre, Malaviya National Institute of Technology, Jaipur 302017, India
Correspondence to: V. Kumar (E-mail: vkt.mnit@gmail.com) and K. Awasthi (E-mail: kamlendra.awasthi@gmail.com)

ABSTRACT: An attempt was taken to synthesize two types of polyaniline (PANI) with and without solvent followed by drying in air and vacuum oven conditions resulting different morphologies. The PANIs were prepared by chemical oxidative polymerization and studied with respect to their morphological features. Scanning electron microscopy, thermogravimetric analysis, X-ray diffractometry, Fourier transform infrared spectroscopy, and ultraviolet–visible spectroscopy techniques were used for the characterization studies. The PANI synthesized with a solvent had a mixed morphology (fibrillar and granular), whereas PANI synthesized without a solvent had only a granular morphology. The direct-current electrical conductivities of the samples were evaluated with an electrometer. We observed that the PANIs with mixed morphology (with solvent) were more electrically conducting than those with a single morphology (without solvent). On drying *in vacuo*, the conductivity of PANI decreased from 3.3×10^{-2} to 0.3×10^{-2} S/cm with solvent treatment, whereas it decreased from 0.1×10^{-2} to 0.3×10^{-3} S/cm without solvent treatment. © 2016 Wiley Periodicals, Inc. J. Appl. Polym. Sci. **2016**, *133*, 44091.

KEYWORDS: conducting polymers; microscopy; morphology; thermogravimetric analysis (TGA)

Received 17 March 2016; accepted 11 June 2016
DOI: 10.1002/app.44091

INTRODUCTION

Conducting polymers are being studied extensively because of their electrical, thermal, and optical properties, which can be exploited in organic electronics.[1] The electrical conductivity of intrinsically conducting polymers depends on the nature of the dopant used, the oxidant to monomer concentration ratio, and the temperature during synthesis. Keeping these points in view, one can easily control or design materials through chemical processing.[2,3] Polyaniline (PANI) has attracted much attention during the last decade because of its chemical and environmental stability,[4] the presence of reactive NH— groups in its polymer chains,[5] and its good electrical conductivity.[6–8] PANI has three idealized oxidation states: the fully reduced state (leucoemeraldine), the fully oxidized state (pernigraniline), and the partially oxidized state (emeraldine). The conductivity of the emeraldine salt form approaches the value of common semiconductors (conductivity = 10^{-4} to 10^{2} S/cm), which exceeds the value of common polymers (conductivity < 10^{-12} S/cm). In this scenario, PANI nanofibers are attractive to researchers because of their unique electrical and mechanical properties. Nanofibers are prepared by the control of the polymerization process via static and dynamic light-scattering measurements. The formation of seeds just before polymerization leads to PANI with a fibrillar morphology.[9] PANI has potential applications in various areas, including displays and electronic devices[10] and in the control of electromagnetic radiation. The use of polymers in electronic devices requires a high level of electrical conductivity. So, it is essential to find an appropriate route for the preparation of the polymer to improve the electrical conductivity. One-dimensional nanofibers have the good advantages of high values of conductivity and surface modification.[11] Various conducting polymers have been reported through different methodologies.[12–20]

There are more ways to synthesize PANI, for example, electrochemical polymerization,[21] template polymerization, enzymatic polymerization or photopolymerization of aniline,[22] interfacial polymerization, and chemical polymerization.[23] Chemical polymerization is cost effective for commercial mass production,[24] easy to use, and comparatively less time consuming. Electrochemical polymerization is expensive and not suitable for mass production. Xiong *et al.*[25] synthesized PANI microtubes via template polymerization. With this approach, the desired shape

of the material was achieved, but it required a most tedious process to eliminate the template, and the polymer could be destroyed during this process.[26,27] An enzymatic polymerization method was used by Zemel and Quinn[28] for the synthesis of PANI. In this method, the reactions taking place at pH values greater than 6.0 resulted in low-conducting PANI.[29] Barros *et al.*[30] used photopolymerization to synthesize PANI composites and observed that the morphology of the conducting polymer depended on the excitation wavelength (granular morphology for ultraviolet synthesis and fibrillar morphology for visible-light excitation). Huang and Kaner[31] synthesized PANI nanofibers without the use of any template. The previously reported methods are expensive and time consuming. The synthesis of PANI via a chemical route involves the mixing of the monomer with an oxidizing agent in aqueous, nonaqueous, or acidic media. A silver nitrate oxidant was used by Sapurina and Stejskal[32] to polymerize aniline via chemical polymerization. It was revealed that the product contained nonconducting aniline oligomers or conducting PANI with a high molecular weight. Liu and coworkers[33,34] synthesized hydrochloric acid (HCl) doped PANI with ammonium peroxodisulfate [$(NH_4)_2S_2O_8$ or APS] as an oxidant and observed a beltlike morphology stacked by spherical particles. The morphology of the polymer depended on the dopant and could be altered by suitable dopants and further tuned by the drying conditions.

However, only few reports are available on the effect of different drying conditions on the morphology of PANI. To best of our knowledge, the preparation of PANI nanofibers with the addition of aniline into an APS solution and the effect of the drying conditions on the morphology and direct-current (dc) electrical conductivity has not been studied so far. In this study, PANI was prepared and dried in different environments in air and in a vacuum to observe the effects on the morphology. Reverse addition of the aniline monomer was carried out in the APS solution to prepare nanofibers. Consequently, the effect of the drying conditions on the dc electrical conductivity of PANI was also investigated in detail. We anticipated that the morphology of PANI would not only depend on the preparation route but also on the drying conditions.

EXPERIMENTAL

PANI was synthesized with and without solvent and was then dried in air and in a vacuum oven. To prepare PANI, deionized water was used as a solvent. The oxidizing agent APS was used because of its high oxidation potential (2.01 V);[32] this, in turn, accelerated the polymerization mechanism. A previous study[33] revealed that PANI prepared with APS oxidant (with solvent) exhibited a granular morphology. The experimental density of the synthesized PANIs was measured with an ME-DNY-4 density kit (Mettler Toledo) according to eq. (1), which works on the basis of Archimedes' principle:

$$\text{Experimental density} = [A/A - B(\rho_0 - \rho_L) + \rho_L] \quad (1)$$

where A and B are the weights of PANI in air and in the distilled water medium, respectively, and ρ_0 and ρ_L are the densities of the distilled water medium (i.e., 0.9967 g/cm^3) and air (i.e., 0.0012 g/cm^3), respectively. After preparation of these materials, further characterizations was done.

Information related to the crystallinity and phases present in the sample was collected with the help of X-ray diffractometry (XRD; PaNalytical X'Pert Pro, Cu Kα radiation, wavelength = 1.54 Å). The XRD data were collected in the 2θ range from 10 to 60° (step size = 0.02° with a scanning rate of 0.7 s). From the XRD pattern, the total area could be divided into crystalline and amorphous components. The degree of crystallinity (X_c) was determined as the ratio of the crystalline area to the total area, as indicated in eq. (2)[35]:

$$X_c(\%) = [A_c/(A_c + A_a)] \times 100 \quad (2)$$

where A_c is the area of the crystalline phase and A_a is the area of the amorphous phase.

The bonding characteristics and absorption spectra of all of the samples were studied with Fourier transform infrared (FTIR) spectroscopy (PerkinElmer, 2000–600 cm^{-1}) and ultraviolet–visible spectroscopy (C60, Agilent Technologies, 300–900 nm), respectively. The PANI samples were prepared in a 1-methyl-2-pyrrolidinone (NMP) solvent for the absorption study. Morphological and thermal characterization was performed with field emission scanning electron microscopy (Nano 450, FEI) and thermogravimetric analysis (TGA; STA 6000, PerkinElmer). TGA was operated in the temperature range from 30 to 650 °C under an N_2 atmosphere at a heating rate of 10 °C/min for thermal study. Furthermore, the pellets (2 mm thick and 13 mm in diameter) were prepared with a hydraulic press (under a pressure of 70 MPa for 4 min), and current–voltage measurements were carried out with an electrometer (2601B, Keithley) in the voltage range −5 to 5 V. The dc electrical resistance of the pellets was measured at room temperature by a standard two-probe method. The dc electrical conductivity of the prepared PANI was calculated with eqs. (3) and (4)[36]:

$$\rho = RA/L \quad (3)$$

$$\text{Conductivity} = 1/\rho \quad (4)$$

where ρ is the resistivity of the PANI pellet, R is the resistance of the PANI pellet, A is the area of the pellet, and L is the thickness of the PANI pellet.

Synthesis of PANI

The following conditions were used: aniline ($C_6H_5NH_2$; 99% purity, Merck) as a monomer, APS (98% purity, Merck) as an oxidant, HCl (37% purity, Merck) as a dopant, and NMP (99% purity, Alfa Aesar). Aniline was doubly distilled before use, whereas the other reagents were used as received. In the presence of solvent, PANI was synthesized by the chemical polymerization of the aniline monomer. A solution of APS (4.564 g) was prepared in 200 mL of 2.5 *M* HCl. Distilled aniline (4 mL) was added to the previous solution for complete solubility of the monomer[37] and stirred vigorously in a chemical bath kept below 5 °C. A volume of 2 mL of aniline was added dropwise (one drop every 10 s), whereas the remaining 2 mL was added at once. The pH of the solution was maintained in acidic medium (pH < 3). The solution was stirred in an airtight flask for another 3 h, and after that, it was left for 10–12 h at room

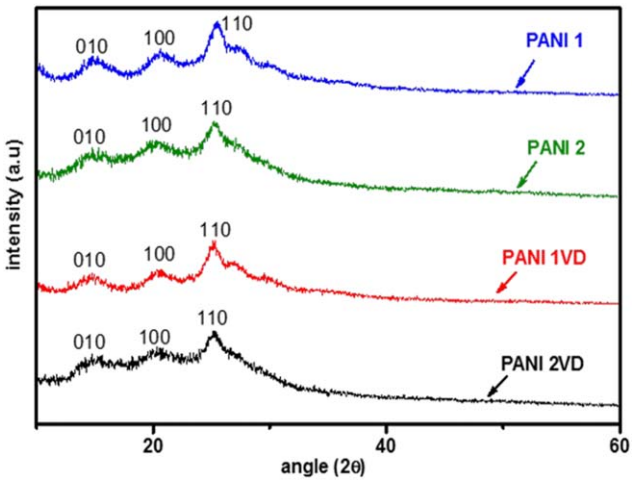

Figure 1. XRD patterns of PANI 1, PANI 1VD, PANI 2, and PANI 2VD. [Color figure can be viewed in the online issue, which is available at wileyonlinelibrary.com.]

temperature to completely polymerize aniline.[38] During polymerization, the color of the solution gradually turned green. The solution was filtered and washed with deionized water to remove the unreacted soluble component with a 0.1 *M* HCl solution to eliminate the unreacted aniline monomer and finally with acetone to remove water. The precipitate was dried separately in air (PANI 1) and in a vacuum oven at 90 °C (PANI 1VD) for 18 h.

The synthesis of PANI without solvent was also done by chemical polymerization. First, distilled aniline (4 mL) was poured into a porcelain mortar, and HCl (2.4 mL) was added dropwise; this was followed by simultaneous grinding (a white paste was formed during this process) for 10 min at room temperature. Subsequently, fine APS powder (11.409 g) was added slowly (to prevent overheating due to the highly exothermic reaction).[39,40] After the addition of APS, the color of the paste changed from white to green; this confirmed the doping of HCl. This paste was transferred into a 2-L beaker containing a solution of acetone, ethanol, and deionized water in a 1:1:8 ratio and left for 1 h. To eradicate the oligomer impurities, the previous solution was washed with deionized water, acetone, and ethanol, respectively, until the brown filtrate became colorless, as also reported by Tantawy *et al.*[3] The obtained product was dried separately in air (PANI 2) and, thereafter, in a vacuum oven at 90 °C (PANI 2VD) for 18 h.

RESULTS AND DISCUSSION

The experimental densities of PANI 1, PANI 2, PANI 1VD, and PANI 2VD were found to be 1.327, 1.331, 1.361, and 1.335 g/cm^3, respectively; these were very close to the density of the commercially available PANI (i.e., 1.36 g/cm^3). The density of the vacuum-dried PANI 2VD was slightly higher than that of the air-dried PANI 2. However, the higher density of PANI 1VD compared to PANI 1 may have been due to the removal of defects and free volume. Another reason may have been the good ordering of the polymeric chain and the change in the molecular weight of the polymers processed under different conditions. The molecular weight of PANI prepared in solvent could be on higher side because of air and moisture; this could have led to an enhancement in the density after the vacuum treatment. It was reported that high-molecular-weight PANI could be achieved when it was prepared below room temperature.[41]

The analysis of XRD patterns (Figure 1) confirmed the formation of PANI and the percentage crystallinity. The three main peaks observed at 2θ values of 14.2, 20.2, and 25.2° corresponded to (010), (100), and (110) crystal planes (JCPDS 00-060-1167) of PANI salt.[3] Peaks of relatively lower intensity at 27.3 and 30° were also observed in PANI 1 and PANI 1VD. It was evident from the XRD data that PANI prepared with a solvent had a greater extent of crystallinity. This may have been due to the orientation of polymeric chains during solution evaporation;[42] this, in turn, produced larger crystalline domains embedded in the amorphous region. We found that the crystallinity of PANI decreased slightly during the vacuum-drying treatment. The percentage crystallinity values for PANI 1, PANI 1VD, PANI 2, and PANI 2VD were calculated as approximately 45, 38, 20, and 15, respectively. These changes in crystallinity were due to the loss of dopant,[43] which was confirmed from FTIR spectroscopy.

The FTIR spectra (Figure 2) of the PANIs were analyzed to confirm the presence of dopant in the air- and vacuum-drying conditions. As expected, the crystallinity of the vacuum-dried PANI was lower compared to that of the air-dried PANI. This change in the crystallinity significantly affected the intensity of the vibrations. The band at 1292 and 1245 cm^{-1} assigned to the bending vibrations of C—N for aromatic amines and C—N$^+$• stretching vibrations in the polaron structure represented the existence of conducting protonated PANI.[36,44] The moisture content in the polymer was measured with the vibrations at 1620 cm^{-1} in their FTIR spectra.[45] The characteristic peaks at 1564 and 1490 cm^{-1} represented C=C stretching of quinoid (N=Q=N) and benzenoid (N=B=N) rings, respectively.[46] The strong band at 1143 cm^{-1} was attributed to the vibration mode of the —NH$^+$= structure and/or C—H in-plane bending

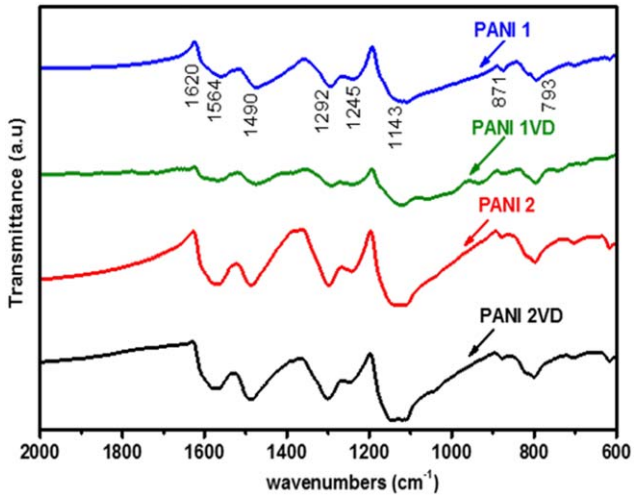

Figure 2. FTIR spectra of PANI 1, PANI 1VD, PANI 2, and PANI 2VD. [Color figure can be viewed in the online issue, which is available at wileyonlinelibrary.com.]

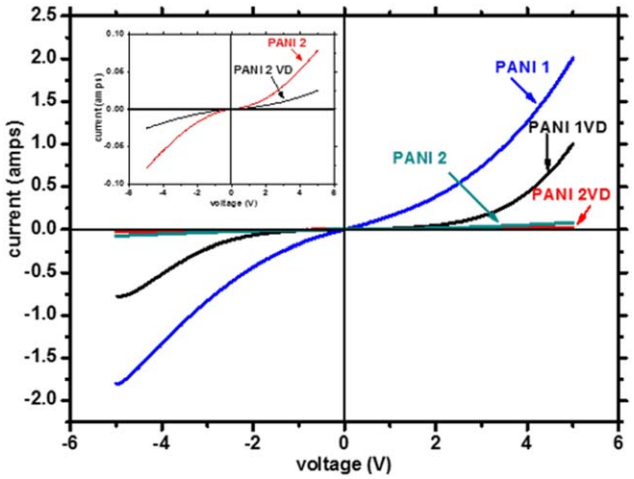

Figure 3. Current–voltage characteristics of PANI 1, PANI 2, PANI 1VD, and PANI 2VD. [Color figure can be viewed in the online issue, which is available at wileyonlinelibrary.com.]

vibrations.[47] The bands observed at 871 and 793 cm^{-1} and corresponding to ring deformation were related to the C—H out-of-plane bending vibrations of the benzene ring.[48] There was no obvious change in the characteristic peaks of any of the PANIs; however, the intensity changed as follows: PANI 2 > PANI 2VD > PANI 1> PANI 1VD. The decrease in the intensity was due to the removal of a small amount of HCl dopant from PANI with the vacuum-drying treatment.[49] For instance, the intensity of the band at 1143 cm^{-1} was higher in the case of PANI (without solvent); this was ascribed to the higher degree of protonation in the backbone due to concentrated acidic medium. This resulted in a higher degree of electron delocalization. The higher degree of protonation may have increased the electrical conductivity of PANI.[50]

The current–voltage characteristics of PANI 1, PANI 2, PANI 1VD, and PANI 2VD are shown in Figure 3 and indicate their cubical parabolic nature at room temperature. The electrical conductivity values of PANI 1 and PANI 1VD were greater than those of PANI 2 and PANI 2VD. However, the degrees of electron delocalization in PANI 2 and PANI 2VD were greater than those of PANI 1 and PANI 1VD. This contradiction could be explained on the basis of the mixed (granular and fibrillar) morphology of PANI 1 and PANI 1VD. An enlarged view of the current–voltage characteristics of PANI 2 and PANI 2VD are shown in the inset. The values of the dc electrical conductivity of PANI 1, PANI 2, PANI 1VD, and PANI 2VD were calculated as 3.3×10^{-2}, 0.1×10^{-2}, 0.3×10^{-2}, and 0.3×10^{-3} S/cm, respectively (Table I). The higher conductivity of PANI 1 may have been due the presence of hairlike nanofibers, moisture content, and strong interior intrachain interactions.[51] In addition, the crystallinity of PANI 1 was higher than the values of 7, 25, and 30% for PANI 1VD, PANI 2, and PANI 2VD, respectively. The higher the crystallinity was, the fewer the number of defects were in the polymer, and this resulted in an enhancement in the conductivity. The reduced resistance of the nanofibers facilitated the drifting of the charge carriers. On vacuum treatment, the slight decrease in the conductivity of PANI 1VD may have been due to the removal of moisture and the formation of branched nanofibers. The branching of nanofibers enhanced the separation, and this reduced interior intrachain interactions and coupling between the polymeric chains.[52] The lower conductivity of PANI 2 and PANI 2VD may have been due to the irregularly shaped granular morphology and less contact between the monomer and oxidant molecule; this may have decreased the oxidation level in PANI prepared without solvent. The weak secondary bonding separated the particle phase, and this may have also favored the decline in the dc electrical conductivity of PANI. Riaz *et al.*[53] reported that irregular agglomerates decreased the desired properties of the polymer. The dc electrical conductivities of one-dimensional/two-dimensional structures are generally greater than those of their three-dimensional counterparts.

The microstructures of the PANIs in air- and vacuum-drying conditions are shown in Figure 4(a–d). PANI prepared with a solvent had a dual morphology {PANI 1 [hairlike nanofibers and a granular morphology see Figure 4 (a and e)] or PANI 1VD (branched nanofibers and a granular morphology)}, whereas PANI prepared without a solvent had only a granular morphology see Figure 4 (c-d). The formation of nanofibers along with grains observed without the addition of any structural directing agent was very interesting and might be the natural morphology of PANI.[54] Such a mixed morphology has rarely been reported in the literature. The reason for the dual morphology in the case of PANI 1 might have been the rate of addition of aniline. Initially, 2 mL of reagent was added dropwise; this formed nanofibers. The remaining 2 mL was added at a once, and this produced the granular morphology.[9,55] Figure 4(b) reveals the branched nanofiber network along with a granular structure for PANI 1VD. On removal of a small amount of HCl dopant, as confirmed by the FTIR spectra, intermolecular hydrogen bonding occurred in PANI, and this resulted in the branching of nanofiber networks.[52,53] The confirmation of the removal of the HCl dopant was also done by TGA. The hairlike nanofibers may have increased the free volume and, hence,

Table I. Morphology, dc Electrical Conductivity, and Band Gaps of the Prepared PANI 1, PANI 2, PANI 1VD, and PANI 2VD

Material	Oxidizing agent	Morphology	Conductivity	Band gap
PANI 1	APS	Hairlike nanofibers and granular	3.3×10^{-2} S/cm	3.25 and 1.67 eV
PANI 2	APS	Granular	0.1×10^{-2} S/cm	3.24 and 1.68 eV
PANI 1VD	APS	Branched nanofibers and granular	0.3×10^{-2} S/cm	3.27 and 1.67 eV
PANI 2VD	APS	Granular	0.3×10^{-3} S/cm	3.20 and 1.63 eV

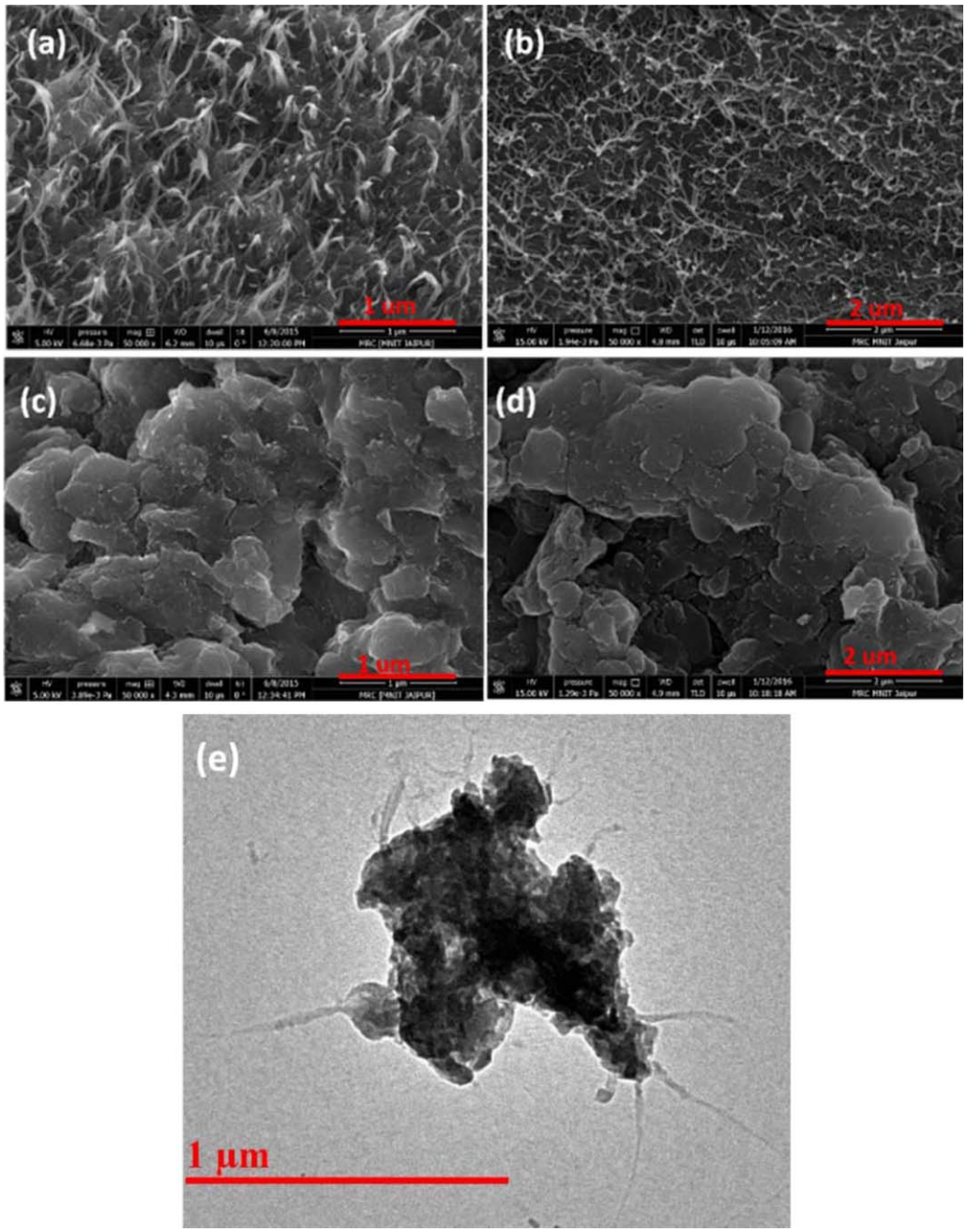

Figure 4. Scanning electron microscopy images of (a) PANI 1, (b) PANI 1VD, (c) PANI 2, and (d) PANI 2VD and (e) transmission electron microscopy image of PANI 1. [Color figure can be viewed in the online issue, which is available at wileyonlinelibrary.com.]

decreased the density of the materials. In the case of PANI prepared without a solvent, the irregularly shaped grains were interconnected well with each other, and this represented a sufficient binding energy to combine with nearby grains or molecules.[56]

Growth Mechanism of the PANI Nanofibers and Granular Structure

The dropwise addition of the aniline monomer into the oxidant solution enhanced its solubility to a larger extent, and this led to the formation of nanofibers. The complete solubility of the monomer formed primary nanofibers, and the secondary chain growth of the nanofibers was suppressed. Wang and Jing[57] reported that a depleted region of oligomeric intermediate and aniline cation was created that surrounded the PANI nanofibers; this assisted the growth and elongation of the nanofibers in one direction because their ends extended to the less depleted region. In addition, the lower nucleation site on the surface of the PANI nanofibers also confirmed the continuity of the PANI nanofibers at the end of polymerization.

In the case of PANI prepared without a solvent, the reactions mainly occurred at the surface of the solid-state reactant. The reported literature shows that the morphology of a product

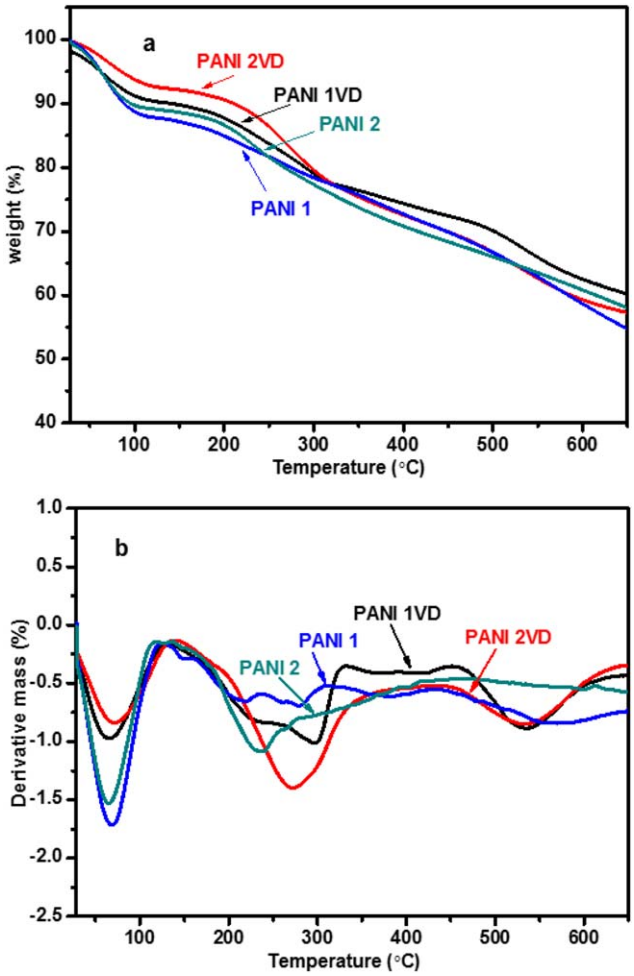

Figure 5. (a) TGA and (b) DTG curves of PANI 1, PANI 1VD, PANI 2, and PANI 2VD. [Color figure can be viewed in the online issue, which is available at wileyonlinelibrary.com.]

generally depends on the rates of nucleation and growth of the product. The interdiffusion rate of the reactant was very slow; this may have been due to less contact between the monomer and oxidant molecules. This may have weakened the secondary bonding (van der Waals interactions) and favored the phase separation of the particles.

Morphology of PANI Changed from a One-Dimensional Shape to a Granular Shape

The dropwise addition of aniline into APS produced clean nanofibers at the early stage of the polymerization process. The initially formed nanofibers acted as nucleation centers for the further precipitation of PANI. With the extreme surplus of APS, the nanofibers became thicker and coarser, and this led to irregularly shaped agglomerates. The relative fraction of nanofibers and granular particles depended on the ability to separate the formation of nanofibers from the secondary growth of the polymer.

The TGA and differential thermogravimetry (DTG) curves of the PANI samples are depicted in Figure 5(a,b). A three-step weight loss process was evident in the TGA curve of the pure PANI. Three major minima were observed in the DTG curve, which showed the majority weight loss of the respective steps.[58–60] The initial weight loss about 100 °C was attributed to the loss of small amounts of absorbed water and unreacted monomers.[61] The second weight loss between 150 and 300 °C was believed to have been due to the decomposition of dopant and low-molecular-weight oligomer.[62,63] We observed that the third weight loss started close to 400 °C, and it was ascribed to the degradation and decomposition of the backbone units of PANI.[64,65] The degradation of the PANI backbone units resulted in the formation of substituted aromatic fragments and the extended aromatic fragment, as confirmed by the bands at 871 and 793 cm^{-1} in the FTIR spectra. Figure 5(a) reveals that there was a lower content of moisture and dopant expelled from the polymeric chains in the vacuum-treated PANIs compared to those that were air dried. The onset temperature is the temperature up to which a material has thermal stability. For PANI 1, PANI 1VD, PANI 2, and PANI 2VD, the onset temperatures were 520, 510, 530, and 515 °C, respectively (Table II). The main decomposition temperature and residual weight values for PANI 1, PANI 1VD, PANI 2, and PANI 2VD were 560 °C and 54.72%, 565 °C and 60.18%, 550 °C and 58.03%, and 555 °C and 57.38%, respectively. The order of moisture percentage, as observed in Figure 5(a), was as follows PANI 1 > PANI 2 > PANI 1VD > PANI 2VD. The higher percentage of moisture content in PANI 1 and PANI 2 compared to PANI 1VD and PANI 2VD, respectively, showed the higher value of dc electrical conductivity. Bellucci *et al.*[66] reported that in the presence of moisture, the electrical conductivity of polyimide increased. A very slight change in the percentage of counter ion of the dopants moieties (Cl^-) may have also affected the mobility of the charge carrier. Hammo[67] reported that a higher electron affinity and lower thermal conductivity in the dopant counter ion (Cl^-) increased the conductivity of PANI. The presence of moisture could have enhanced the electrical conductivity of PANI. Among all of the PANIs, PANI 1 showed a higher content of moisture, and this resulted in a higher conductivity compared to those observed in the others.

To prove the presence of benzenoid and quinoid rings in the PANI samples, absorption spectra (Figure 6) were recorded. The spectra were taken in NMP solvent; this turned the color of PANI from green to blue (i.e., indication of the conversion of emeraldine salt to emeraldine base). There were no changes in the absorption spectra of all of the samples; this may have been

Table II. Calculation of the Onset Temperature, Decomposition Temperature, and Char Percentage of the Prepared PANI 1, PANI 2, PANI 1VD, and PANI 2VD

Material	Onset temperature (°C)	Decomposition temperature (°C)	Char (%)
PANI 1	520	560	54.72
PANI 2	530	550	58.03
PANI 1VD	510	565	60.18
PANI 2VD	515	555	57.38

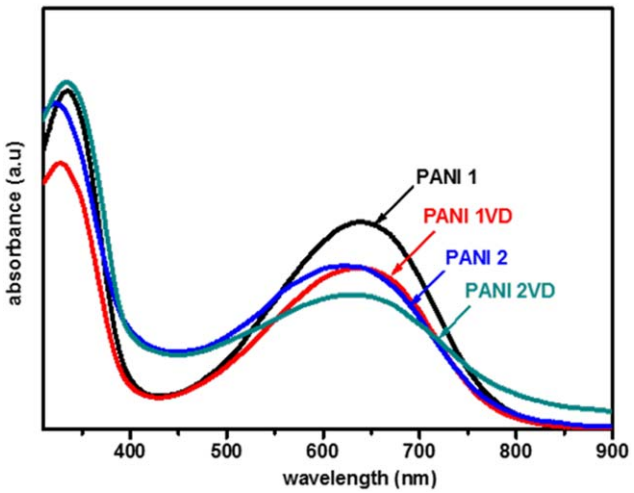

Figure 6. Absorption spectra of PANI 1, PANI 1VD, PANI 2, and PANI 2VD. [Color figure can be viewed in the online issue, which is available at wileyonlinelibrary.com.]

due to the same dopant used during the preparation of PANI. Babu *et al.*[68] reported that PANI prepared with various oxidants had different absorptions. The absorption spectra showed intense and broad absorptions at 330 and 630 nm; this confirmed the formation of emeraldine base.[69] The absorption at 330 nm might have been correlated with the π–π* transition within benzenoid rings, that is, the electronic transition from highest occupied molecular orbital to lowest unoccupied molecular orbital, and the absorption at 630 nm should have been π–π* transitions within the quinoid rings.[70,71] The intensity of the peak corresponding to the quinoid ring was relatively weak because the addition of HCl into the PANI backbone changed electron delocalization into the polymeric chains and led to charge equalization. The equalization of charge formed the conjugated system, and protonation occurred at the imine ion of the quinoid ring; this generated the excited polaron.[72] The optical band gap (E_g) of the synthesized materials was calculated by Tauc's relation:[73]

$$(\alpha h\upsilon) = B(h\upsilon - E_g)^n \quad (5)$$

where B is a constant, α is the absorption coefficient, h is Planck's constant (6.625×10^{-34} J s), and υ is the frequency of the incident photon. The exponent n has discrete values of 1/2, 3/2, 2, and 3, and $n = 1/2$ is assigned to direct allowed transitions, $n = 3/2$ is assigned to direct forbidden transitions, $n = 2$ is assigned to indirect allowed transitions, and $n = 3$ is assigned to indirect forbidden transitions. The Tauc plot for the calculation of the optical band gap (with respect to both peaks) is shown in Figure 7(a,b). Extrapolation of tangent on both the peaks, obtained in the absorption spectra, indicated values of the optical band gap of 3.25 and 1.67 eV (PANI 1), 3.24 and 1.68 eV (PANI 2), 3.27 and 1.67 eV (PANI 1VD), and 3.20 and 1.63 eV (PANI 2VD). The observed data for both PANIs are summarized in Table I. Our results suggest that the morphological and physical properties of PANI could be improved through the selection of an appropriate route of preparation.

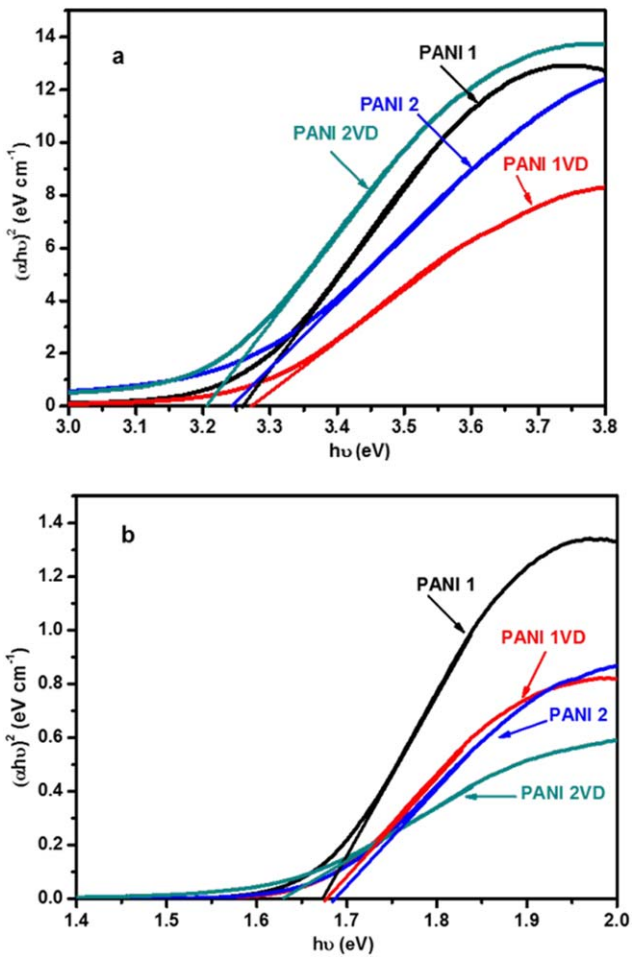

Figure 7. Optical band gaps of PANI 1, PANI 1VD, PANI 2, and PANI 2VD. [Color figure can be viewed in the online issue, which is available at wileyonlinelibrary.com.]

CONCLUSIONS

PANI was prepared via two routes (with and without solvent), and this was followed by air or vacuum oven treatment. The PANIs prepared with a solvent had a dual morphology (hair-like/branched nanofibers and granular), whereas the PANIs prepared without solvent exhibited only a granular morphology. The dual morphology in the solvent-treated PANI was attributed to the slow rate of addition of the aniline monomer. The solvent-treated PANIs were more crystalline in nature than they were without solvent. Thermograms revealed that the vacuum-dried PANIs had less moisture and HCl dopant. The current–voltage curves suggested that solvent-treated PANIs were more conducting than without solvent; this might have been due to the presence of nanofibers and the lower moisture content.

ACKNOWLEDGMENTS

The authors thank the Materials Research Centre (Malaviya National Institute of Technology, Jaipur, India) for providing the characterization facilities. They also acknowledge the financial support of the Department of Science and Technology (New Delhi, India). Kamlendra Awasthi and Manoj Kumar acknowledge the financial support of an Innovation in Science Pursuit for Inspired Research faculty award from the Department of Science and Technology. Thanks go to Karina Khan (Jayoti Vidyapeeth Women's

University, Jaipur, India) for her help during synthesis. The authors further extend thanks to P. K. Sain (lecturer in physics, Government Polytechnic College, Bharatpur, India) and Akash Katoch (Indian Institute of Technology, Roorkee, India) for their valuable suggestions.

REFERENCES

1. Cao, G. Nanostructures and Nanomaterials: Synthesis, Properties and Applications Imperial College Press: London, **2004**.
2. Joo, J.; Epstein, A. *J. Appl. Phys. Lett.* **1994**, *65*, 2278.
3. Tantawy, H. R.; Aston, D. E.; Smith, J. R.; Young, J. L. *ACS Appl. Mater. Interfaces* **2013**, *5*, 4648.
4. Kumar, A.; Jangir, L. K.; Kumari, Y.; Kumar, M.; Kumar, V.; Awasthi, K. *Macromol. Symp.* **2015**, *357*, 229.
5. Mostafaei, A.; Zolriasatein, A. *Prog. Nat. Sci. Mater. Int.* **2012**, *22*, 273.
6. Tilki, T.; Karabulut, O.; Yavuz, M.; Kaplan, A.; Cabuk, M.; Takanoglu, D. *Mater. Chem. Phys.* **2012**, *135*, 563.
7. Reddy, K. R.; Sin, B. C.; Ryu, K. S.; Noh, J.; Lee, Y. *Synth. Met.* **2009**, *159*, 1934.
8. Reddy, K. R.; Lee, K. P.; Gopalan, A. I.; Kim, M. S.; Showkat, A. M.; Nho, Y. C. *J. Appl. Polym. Sci.* **2006**, *44*, 3355.
9. Zhang, B. X.; Kolla, H. S.; Wang, X.; Raja, K.; Manohar, S. K. *Adv. Funct. Mater.* **2006**, *16*, 1145.
10. Jia, W.; Segal, E.; Kornemandel, D.; Lamhot, Y.; Narkis, M.; Siegmann, A. *Synth. Met.* **2002**, *128*, 115.
11. Im, J. S.; Kim, S. J.; Kang, P. H.; Lee, Y. S. *J. Ind. Eng. Chem.* **2009**, *15*, 699.
12. Ojani, R.; Raoof, J. B.; Zamani, S. *Talanta* **2010**, *81*, 1522.
13. Reddy, K. R.; Park, W.; Sin, B. C.; Noh, J.; Lee, Y. *J. Colloid Interface Sci.* **2009**, *335*, 34.
14. Reddy, K. R.; Lee, K. P.; Gopalan, A. I. *J. Nanosci. Nanotechnol.* **2007**, *7*, 3117.
15. Reddy, K. R.; Sin, B. C.; Ryu, K. S.; Kim, J. C.; Chung, H.; Lee, Y. *Synth. Met.* **2009**, *159*, 595.
16. Zhang, Y. P.; Lee, S. H.; Reddy, K. R.; Gopalan, A. I.; Lee, K. P. *J. Appl. Polym. Sci.* **2007**, *104*, 2743.
17. Reddy, K. R.; Hassan, M.; Gomes, V. G. *Appl. Catal. A* **2015**, *489*, 1.
18. Reddy, K. R.; Lee, K. P.; Gopalan, A. I.; Showkat, A. M. *Polym. Adv. Technol.* **2007**, *18*, 38.
19. Reddy, K. R.; Lee, K. P.; Lee, Y.; Gopalan, A. I. *Mater. Lett.* **2008**, *62*, 1815.
20. Hassan, M.; Reddy, K. R.; Haque, E.; Faisal, S. N.; Ghasemi, S.; Minett, A. I.; Gomes, V. G. *Compos. Sci. Technol.* **2014**, *98*, 1.
21. Karami, H.; Asadi, M. G.; Mansoori, M. *Electrochim. Acta* **2012**, *61*, 151.
22. Bhadra, S.; Khastgir, D.; Singha, N. K.; Lee, J. H. *Prog. Polym. Sci.* **2009**, *34*, 783.
23. Tran, H. D.; Darcy, J. M.; Wang, Y.; Beltramo, P. J.; Strong, V. A.; Kaner, R. B. *J. Mater. Chem.* **2011**, *21*, 3534.
24. Toshima, N.; Hara, S. *Prog. Polym. Sci.* **1995**, *20*, 155.
25. Xiong, S.; Wang, Q.; Xia, H. *Synth. Met.* **2004**, *146*, 37.
26. Cai, Z.; Martin, C. R. *J. Am. Chem. Soc.* **1989**, *111*, 4138.
27. Wei, Z.; Zhang, Z.; Wan, M. *Langmuir* **2002**, *18*, 917.
28. Zemel, H.; Quinn, J. F. U.S. Pat. 5,420,237 (**1995**).
29. Akkara, J. A.; Kaplan, D. L.; Kurioka, H.; Uyama, H.; Kobayashi, S. *ACS Polym. Mater. Sci. Eng. Conf. Proc.* **1996**, *74*, 39.
30. Barros, R. A.; Azevedo, W. M.; Aguiar, F. M. *Mater. Charact.* **2003**, *50*, 131.
31. Huang, J.; Kaner, R. B. *J. Am. Chem. Soc.* **2004**, *126*, 851.
32. Sapurina, I. Y.; Stejskal, J. *Russ. J. Gen. Chem.* **2012**, *82*, 256.
33. Liu, H.; Wang, Y.; Gou, X.; Qi, T.; Yang, J.; Ding, Y. *Mater. Sci. Eng. B* **2013**, *178*, 293.
34. Katoch, A.; Burkhart, M.; Hwang, T.; Kim, S. S. *Chem. Eng. J.* **2012**, *192*, 262.
35. Soliman, E.; Furuta, M. *Food Nutr. Sci.* **2014**, *5*, 1040.
36. Saini, P.; Choudhary, V.; Singh, B. P.; Mathur, R. B.; Dhawan, S. K. *Mater. Chem. Phys.* **2009**, *113*, 919.
37. Gopta, B.; Prakash, R. *J. Appl. Polym. Sci.* **2009**, *114*, 874.
38. Singh, V.; Mohan, S.; Singh, G.; Pandey, P. C.; Prakash, R. *Sens. Actuators B* **2008**, *132*, 99.
39. Fu, Y.; Elsenbaumer, R. L. *Chem. Mater.* **1994**, *6*, 671.
40. Stejskal, J.; Gilbert, R. G. *Pure Appl. Chem.* **2002**, *74*, 857.
41. Stejskal, J.; Hlavata, D.; Holler, P.; Trchova, M.; Prokes, J.; Sapurina, I. *Polym. Int.* **2004**, *53*, 294.
42. Sain, P. K.; Goyal, R. K.; Prasad, Y. V. S. S.; Jyoti, Sharma, K. B.; Bhargava, A. K. *J. Appl. Polym. Sci.* **2015**, *132*, DOI: 10.1002/app.42443.
43. Begum, A. N.; Dhachanamoorthi, N.; Saravanan, M. E. R.; Jayamurugan, P.; Manoharan, D.; Ponnuswamy, V. *Optik* **2013**, *124*, 238.
44. Gomathi, D. P.; Lee, S. C.; Al-Deyab, S. S.; Lee, S. H.; Ghim, H. D. *J. Ind. Eng. Chem.* **2012**, *18*, 1213.
45. Mirghani, M. S.; Kabbashi, N. A.; Alam, M. Z.; Qudsieh, I. Y.; Alkatib, M. F. R. *J. Am. Oil Chem. Soc.* **2011**, *88*, 1897.
46. Hongxia, J.; Qiaoling, L.; Yun, Y.; Zhiwu, G.; Xiaofeng, Y. *J. Magn. Magn. Mater.* **2013**, *332*, 10.
47. Wang, J.; Wang, J.; Yang, Z.; Wang, Z.; Zhang, F.; Wang, S. *React. Funct. Polym.* **2008**, *68*, 1435.
48. Trchova, M.; Stejskal, J. *Pure Appl. Chem.* **2011**, *83*, 1801.
49. John, H.; Kumar, S. B.; Mathew, K. T.; Joseph, R. *J. Appl. Polym. Sci.* **2002**, *83*, 2008.
50. Tang, T. H.; Jau, Y. N.; Yu, R. P. *Appl. Surf. Sci.* **2012**, *258*, 3184.
51. Wang, Y.; Chen, K.; Li, T.; Li, H.; Zeng, R.; Zhang, R.; Gu, Y.; Ding, J.; Liu, H. *Synth. Met.* **2014**, *198*, 293.
52. Su, B.; Tong, Y.; Bai, J.; Lei, Z.; Wang, K.; Mu, H.; Dong, N. *Indian J. Chem. A* **2007**, *46*, 595.

53. Riaz, U.; Ahmad, S.; Ashraf, S. M. *Nanoscale Res. Lett.* **2008**, *3*, 45.
54. Huang, J.; Kaner, R. B. *Chem. Commun.* **2006**, *28*, 367.
55. Huang, J.; Kaner, R. B. *Angew. Chem. Int. Ed.* **2004**, *43*, 5817.
56. Chanashetty, V. B.; Sharanappa, G.; Patil, B. M.; Sangshetty, K. *Int. J. Eng. Res.* **2013**, *2*, 1.
57. Wang, Y.; Jing, X. *J. Phys. Chem. B* **2008**, *112*, 1157.
58. Wolter, A.; Rannou, P.; Travers, J. P.; Gilles, B.; Djurado, D. *Phys. Rev. B* **1998**, *58*, 7637.
59. Yue, J.; Epstein, A. J.; Zhong, Z.; Gallagher, P. K. *Synth. Met.* **1991**, *41*, 765.
60. Lee, D.; Char, K. *Polym. Degrad. Stab.* **2002**, *75*, 555.
61. Kumar, A.; Mishra, A.; Awasthi, K.; Kumar, V. *Macromol. Symp.* **2015**, *357*, 168.
62. Chan, H. S. O.; Teo, M. Y. B.; Khor, E.; Lim, C. N. *J. Therm. Anal.* **1989**, *35*, 765.
63. Neoh, K. G.; Kang, E. T. *Thermochim. Acta* **1990**, *171*, 279.
64. Wei, Y.; Hsueh, K. F. *J. Polym. Sci. Part A: Polym. Chem.* **1989**, *27*, 4351.
65. Pielichowski, K. *Solid State Ionics* **1997**, *104*, 123.
66. Bellucci, F.; Khamis, I.; Senturia, S. D.; Latanision, R. M. *J. Electrochem. Soc.* **1990**, *137*, 1778.
67. Hammo, S. M. Tikrit, J *Pure Sci.* **2012**, *17*, 1813.
68. Babu, V. J.; Vempati, S.; Ramakrishna, S. *Mater. Sci. Appl.* **2013**, *4*, 1.
69. Zhang, D. *Polym. Test.* **2007**, *26*, 9.
70. Borah, R.; Banerjee, S.; Kumar, A. *Synth. Met.* **2014**, *197*, 225.
71. Stafstrom, S.; Bredas, J. L.; Epstein, A. J.; Woo, H. S.; Tanner, D. B.; Huang, W. S.; MacDiarmid, A. G. *Phys. Rev. Lett.* **1987**, *59*, 1464.
72. Huang, H.; Guo, Z. Preparation and Application of Conductive Polyaniline, 1st ed. Science: Beijing, **2010**; Chapter 4, p 81.
73. Reda, S. M.; Al-Ghannam, S. M. *Adv. Mater. Phys. Chem.* **2012**, *2*, 75.